Hindawi
Advances in Materials Science and Engineering
Volume 2022, Article ID 6576263, 7 pages
https://doi.org/10.1155/2022/6576263

Research Article

Influence of Zinc-Saturated Zeolite on Portland Cement Hydration Kinetics

Damir Barbir and Pero Dabic

Faculty of Chemistry and Technology, University of Split, Split, Croatia

Correspondence should be addressed to Damir Barbir; dbarbir@ktf-split.hr

Received 8 March 2022; Revised 5 July 2022; Accepted 8 July 2022; Published 3 August 2022

Academic Editor: Robert Černý

This work examines the influence of zeolite saturated with zinc (SZ) on the early hydration of Portland cement. The measurements and results indicate that the microcalorimetric method allows continuous observation and determination of SZ's influence on kinetic processes in the early stages of hydration. According to the total heat released after 48 hours of hydration, higher SZ content results in lower heat values, while the maximum hydration occurs earlier. As SZ proportion increases, the rate of heat release and the degree of hydration decrease. Measured hydration degrees differ significantly from the calculated values when SZ is added to Portland cement, especially later in the hydration process.

1. Introduction

Cement production requires a large amount of electricity and is responsible for global CO_2 emissions of 5–8%. CO_2 is produced by the process of calcining limestone and burning fuel in the kilns [1]. One of the most effective methods of reducing greenhouse gas emissions and energy consumption in the cement industry is the partial replacement of cement with silicate and aluminosilicate materials [2]. As most of the supplementary cementitious materials (SCMs) are by-products of various industries, their use will not only reduce CO_2 emissions and energy consumption but also prevent the disposal of these materials in the environment [3–5]. Furthermore, the use of SCMs has a positive effect on the properties of fresh and hardened concrete. Indeed, some SCMs improve the workability of fresh concrete, reduce leaching, and delay the setting time, which is particularly important in areas with high temperatures [6].

Zeolites are crystalline hydrated aluminosilicates of alkali and alkaline earth elements [7]. Recently, natural and modified zeolites have become very popular due to their ability to bind heavy metals and radioactive substances. The use of natural zeolites in the treatment of waste water contaminated with heavy metals is an essential aspect of environmental compatibility due to the economic efficiency and the excellent physical and chemical properties of zeolites [8]. Once zeolite is saturated with heavy metals, it becomes a harmful waste itself and should be treated in a way that does not endanger the environment [9]. A practical method of disposing saturated zeolites is to dispose them in a cement matrix [10–12]. However, the effect of zeolite saturated with heavy metals on the hydration process of Portland cement is still not clear.

The hydration of Portland cement is a series of chemical reactions between the clinker minerals, gypsum, and water, which occur simultaneously or at different rates. As the hydration process begins, the cement paste begins to thicken until it finally hardens. The hydration reactions continue until the reactants or the free space for the formation of hydration products disappear [13].

The progress of hydration is reflected in the development of the chemical, physical, mechanical, and electrical properties of the cement paste. Therefore, the progress of hydration can be monitored by measuring changes in chemical composition, enthalpy, ultrasonic velocity, volume changes, and changes in the strength of hardened cement paste [14]. A common method for monitoring the progress of the hydration reactions of Portland cement is to register the heat

development curves [15, 16]. These curves do not provide a representative answer to mechanical questions but are useful to correlate experimental data with respect to an individual parameter, i.e., heat development. The hydration process is exothermic, which allows the monitoring of hydration reactions with calorimetric methods [17, 18]. Years of experience in the field of hydration process analysis of complex disperse systems offer the possibility to extend the application of calorimetric methods in the control of raw material quality and the control of properties of building composites [19, 20].

2. Development of a Mathematical Model for Kinetic Analysis of Portland Cement Hydration

According to the Krstulović–Dabić model, the hydration reaction of the cement composite can be divided into three basic processes, namely: nucleation and crystal growth (NG), interactions at phase boundaries (I), and diffusion (D) [21]. All three processes occur simultaneously, but the slowest determines the speed of the entire hydration process [22]. Therefore, it is necessary to determine the speeds of all three processes. Observations from previous studies suggest that nucleation and crystallization are the slowest processes at first, while interactions at phase boundaries and diffusion become more important over time [23–25].

In the nucleation and growth process, the basic Avrami–Erofeev equation describing hydration kinetics is often used for spherical particles and is represented by [26]

$$\frac{d\alpha}{dt} = n \cdot K_{NR}^{n} \cdot t^{n-1} \cdot e^{-(K_{NR} \cdot t)^{n}}, \quad (1)$$

where α is the reaction degree of reactants, KNR is the nucleation and growth constant, and t is time. The exponent n describes the geometry of crystal growth and usually falls in the range of 1 to 3.

During the second stage of hydration, the hydration reaction slows down, and the total rate is determined by the reaction interactions at the phase boundary, which can be shown by

$$\frac{d\alpha}{dt} = 3 \cdot K_I \cdot (1 - K_I \cdot t)^2, \quad (2)$$

where K_I is the phase boundary interaction constant.

In the third stage of hydration, when the process is further slowed down due to diffusion through the layer of products formed around the anhydride of the cement particle, the total rate is determined by the diffusion process described by the Jander relation:

$$\frac{d\alpha}{dt} = \frac{3}{2} \cdot K_D \cdot \frac{\left(1 - \sqrt{K_D \cdot t}\right)^2}{2 \cdot \sqrt{K_D \cdot t}}, \quad (3)$$

where K_D is the phase boundary interaction constant.

α-t functions are considered the basis for the development of a mathematical model. Differential kinetic forms of the equations are obtained by deriving integral α-t functions, and the integral functions represent partial solutions. Each differential equation describes the change in hydration rate for each individual process defined in the time interval 0-∞. This paper focuses on the influence of zeolite saturated with zinc ions on the hydration kinetics of Portland cement composites and will contribute to the understanding of the hydration mechanism of cement with different additions of saturated zeolite.

3. Experimental

For all investigated samples, an ordinary Portland cement OPC type CEM I 42.5R was used. OPC was purchased from the cement plant CEMEX, Kaštel Sućurac, Croatia. Natural zeolite saturated with zinc ions from the Donje Jesenje site in Croatia was used as supplementary material to the cement. The saturation was performed with a solution containing 9.0 mmol dm-3 $ZnSO_4$. Zeolite contains the main mineral clinoptilolite and impurities such as illite, feldspar, and quartz (Figure 1). The saturated zeolite (SZ) was dried to a constant weight at 60°C, ground, and sieved through a 90 μm sieve. The chemical compositions of OPC and natural zeolites are shown in Table 1. Natural zeolite (NZ) consists of 64.93 wt. % SiO_2 and 13.66 wt.% Al_2O_3 and with such a composition can be classified as a potential pozzolanic material (the composition of silicon and aluminum should be over 70%).

Mix proportions of cement paste are shown in Table 2.

The mark C indicates OPC without addition, while C10SZ, C20SZ, and C30SZ are short for the cement samples containing 10, 20, and 30 wt.% saturated zeolite, respectively. The effect of SZ on hydration processes was determined by a differential microcalorimeter of the conduction-isoperibolic type at 20°C and water/binder ratio (W/B) 0.5. An ALMEMO 2390-8 data logger, Ahlborn, Germany, was used to trace the changes of voltage dU = f(t) due to changes of temperature in the samples during the first 48 hours of hydration. Computer programs calculate total heat released, heat release rate, and relative reaction degree from the measured thermovoltage values.

4. Results and Discussion

Figures 2 and 3 show the curves for hydration heat released rate and total heat of hydration of Portland cement samples with SZ.

Table 3 shows the end of the induction period and the duration of the acceleration period. Table 4 shows the maximum rate of hydration heat released and the total amount of heat released at different hydration times.

Based on Figure 2, all samples undergo similar hydration processes. Comparing the results of the influence of natural zeolite and zeolite saturated with zinc on hydration, both curves retain a similar shape, which indicates that neither natural zeolite nor saturated zeolite affects main hydration mechanisms. In terms of decreasing the amount of heat released and the rate of heat release, saturated zeolite has a greater impact [11, 28]. After mixing binder and water, a very sharp exothermic peak occurs due to the rapid dissolution of the clinker minerals and the rapid formation of

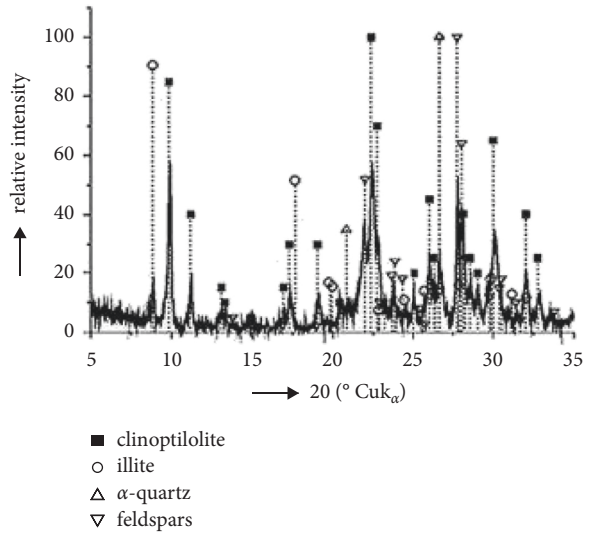

Figure 1: XRD of NZ from Donje Jesenje site, Croatia [27].

Table 1: Chemical compositions of OPC and NZ from Donje Jesenje site.

Compositions, wt. %	SiO_2	Al_2O_3	Fe_2O_3	CaO	MgO	K_2O	Na_2O
OPC	22.9	4.8	2.8	65.2	1.6	1.8	0.2
NZ	64.9	13.7	2.0	3.0	1.1	1.9	3.7

Table 2: Mix proportions of samples.

Sample	Cement, g	Saturated zeolite, g
C	4.0	0.0
C10SZ	3.6	0.4
C20SZ	3.2	0.8
C30SZ	2.8	1.2

ettringite and syngenite. The period after the initial period is the induction period, during which the hydration reaction begins to slow down. This period provides information on the workability time. The heat value drops sharply and remains constant for several hours (Figure 3).

Based on Table 3, sample C (pure Portland cement) requires an induction period of about 3.15 hours, whereas samples C10SZ, C20SZ, and C30SZ require about 2.26, 2.95, and 3.08 hours, respectively. In the hydration acceleration period, the first peak corresponds to the beginning of setting, and the second peak corresponds to the end of setting and the beginning of hardening of the cement paste. As can be seen in Table 3, adding SZ to the cement-water system does not affect the beginning of the acceleration period or the appearance of the main peak. It only affects the intensity of the main peak (by increasing the SZ, there is a decrease in the heat release rate), as can be seen in Figure 2. As a result of the SZ addition to the acceleration period, the Ca2+ ions are deposited on either the surface of the SZ or in the form of a C-S-H gel. The maximum value of the main peak decreases by 23%, from 9.10 J $^{-1}h^{-1}$ to 6.97 J $g^{-1}h^{-1}$ after incorporating 10 wt. % SZ. When the SZ content increases to 20 and 30 wt.

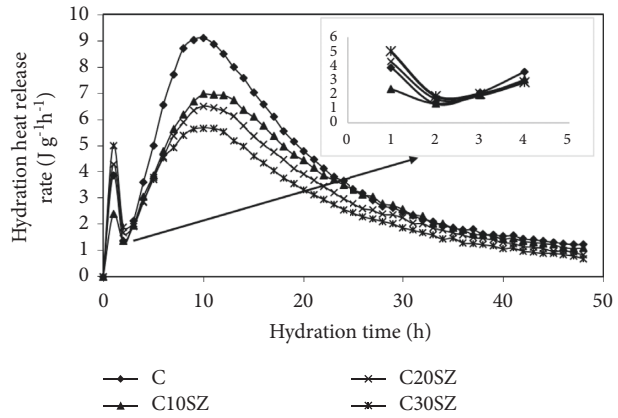

Figure 2: Hydration heat released rate of the Portland cement samples without and with SZ.

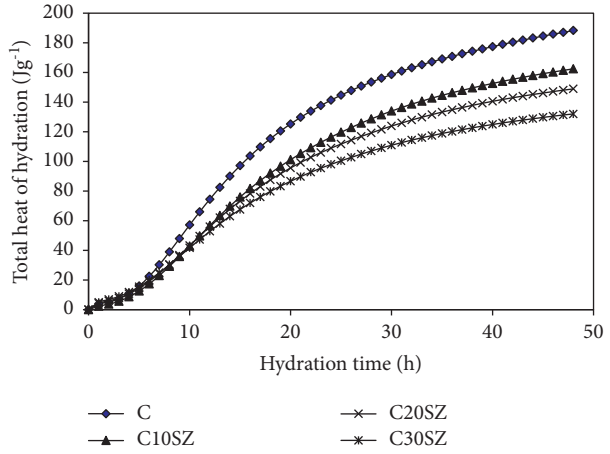

Figure 3: Total heat of hydration of the Portland cement samples without and with SZ.

Table 3: The end of induction period and duration of acceleration period during hydration processes.

	Sample			
	C	C10SZ	C20SZ	C30SZ
The end of induction period, *h*	3.15	2.26	2.95	3.08
Duration of acceleration period, *h*	7.68	9.80	8.56	8.42

%, the maximum value of the main peak is decreased by 6 and 13%, from 6.97 J $g^{-1}h^{-1}$ to 6.52 J $g^{-1}h^{-1}$ and from 6.52 J $g^{-1}h^{-1}$ to 5.67 J $g^{-1}h^{-1}$. The low hydration activity of SZ may be the main affecting factor.

Figure 3 shows that the total heat of hydration decreases with the increase of SZ content. The 12 hours' heat released decreases by 24% from 74.50 J g^{-1} to 56.75 J g^{-1} after addition of 10 wt. % SZ. When the SZ content increases to 20 and 30 wt. %, the heat released decreases by 1% and 6% from 56.75 J g^{-1} to 56.03 J g^{-1} and from 56.03 J g^{-1} to 52.84 J g^{-1}. The 48 hours' heat released decreases by 14%, 8%, and 11% from 188.28 J g^{-1} (C) to 162.52 J g^{-1} (C10SZ), 148.93 J g^{-1} (C20SZ), and 132.04 J g^{-1} (C30SZ).

Table 4: Rate of the second heat released peak and total heat released of samples at 20°C.

Sample	Rate of the second heat released peak, J g^{-1}h^{-1}	Total heat released, J g^{-1}		
		12 h	24 h	48 h
C	9.10	74.50	141.36	188.28
C10SZ	6.97	56.75	116.40	162.52
C20SZ	6.52	56.03	108.96	148.93
C30SZ	5.67	52.84	98.02	132.04

5. Hydration Kinetics Model of Portland Cement-Saturated Zeolite System

The mathematical model is based on the assumption that three processes occur simultaneously on the surface of a cement particle: nucleation and growth, phase boundary interaction, and diffusion. The slowest process controls the overall hydration rate. Using the assumed model, it is possible to estimate the values of the kinetic parameters of the hydration process in the cement-saturated zeolite system. The estimated values of the kinetic parameters are shown in Table 5. Theoretical and experimental hydration curves of the four samples are shown in Figures 4–7.

From Table 5, it can be seen that the value of the nucleation and growth constant (KNR) for sample C (Portland cement without addition) is 0.0480 h^{-1}, and that for samples C10SZ, C20SZ, and C30SZ is 0.0390 h^{-1}, 0.0370 h^{-1}, and 0.0340 h^{-1}. These results indicate that increasing the addition of saturated zeolite slows down the nucleation and growth process. The value of the exponent n for Portland cement without addition (C) is 2.20, while the samples containing saturated zeolite (C10SZ, C20SZ, and C30SZ) have a much lower value of this exponent. This indicates that the addition of saturated zeolite greatly affects the crystal growth geometry. The rate of the phase-boundary interaction process is described by the K_I constant. The value of the K_I constant for sample C is 0.0249 h^{-1}. At lower zeolite addition (C10SZ), the K_I constant assumes a lower value indicating a decrease in the rate of hydration processes when the interaction process at the phase boundary is a controlled process.

Increasing the content of saturated zeolite (C20SZ and C30SZ), the rate of hydration process increases. From the results of determining the transition time of $t_{NR\text{-}I}$ from one controlling process to another (NR⟶I), it is evident that in the system without the addition of saturated zeolite, the transition time is $t_{NR\text{-}I} = 9.47$ h. In a system with the addition of 10 wt. % saturated zeolite, the duration of the NR process is shortened, while the effect of prolonging the duration of NR was observed in the system with increased addition. The process that follows the phase boundary interaction process is the diffusion process, which is described by the K_D constant. To start the diffusion process, the phase boundary interaction process rate and the diffusion rate must be equal. The value of the K_D constant for sample C is 0.0037 h^{-1}, while the addition of saturated zeolite increases the K_D value and it can be concluded that the addition of saturated zeolite increases the diffusion rate. The transition time $t_{I\text{-}D}$ for cement without admixture is 26.84 h, while for samples

Table 5: Kinetic parameters of hydration in the cement-saturated zeolite system.

Kinetic parameter	C	C10SZ	C20SZ	C30SZ
n	2.20	2.09	1.96	1.85
K_{NR}, h^{-1}	0.0480	0.0390	0.0370	0.0340
K_I, h^{-1}	0.0249	0.0235	0.0245	0.0255
K_D, h^{-1}	0.0037	0.0051	0.0062	0.0072
$t_{NR\text{-}I}$, h	9.47	9.21	10.00	10.00
$t_{I\text{-}D}$, h	26.84	28.42	27.63	26.32

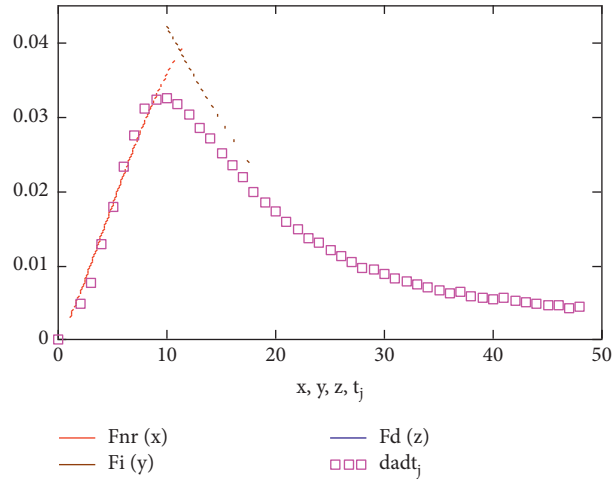

Figure 4: Hydration rate curves of sample C.

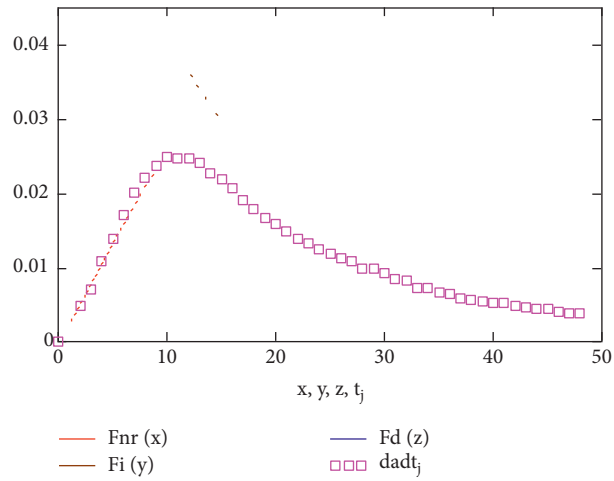

Figure 5: Hydration rate curves of sample C10SZ.

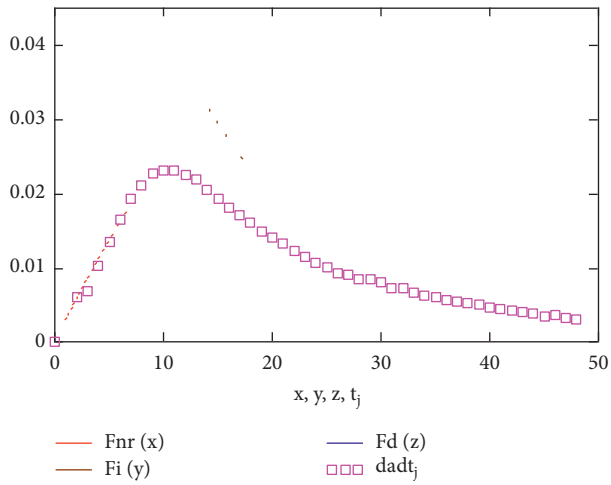

Figure 6: Hydration rate curves of sample C20SZ.

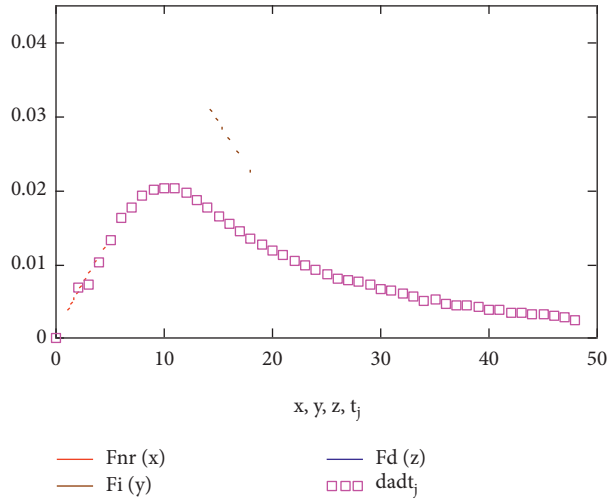

Figure 7: Hydration rate curves of sample C30SZ.

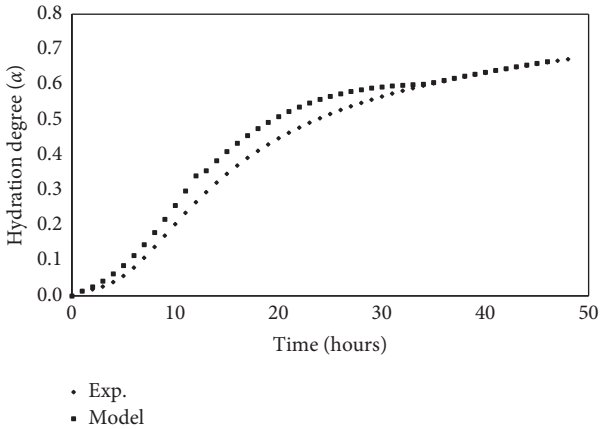

Figure 8: Experimental results of the hydration degree with the assumed kinetic model for sample C.

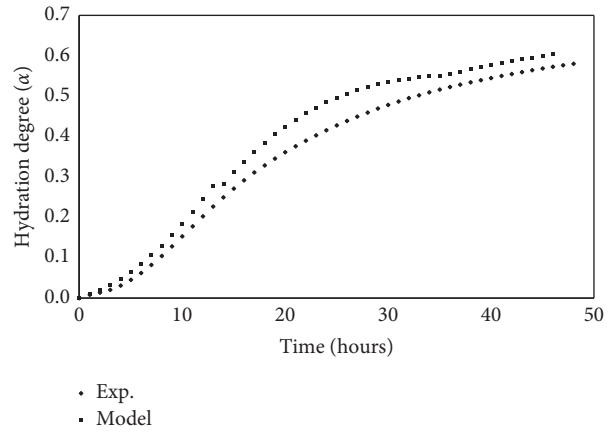

Figure 9: Experimental results of the hydration degree with the assumed kinetic model for sample C10SZ.

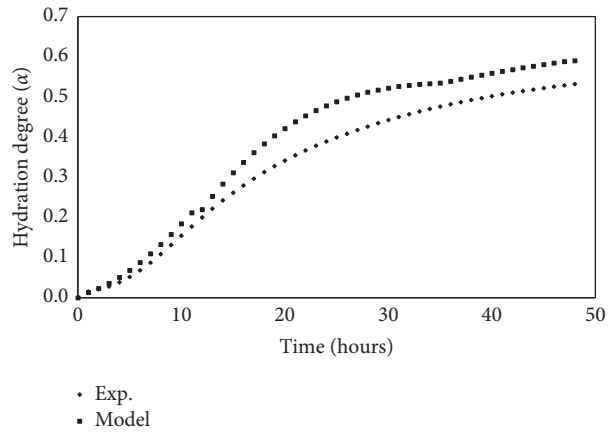

Figure 10: Experimental results of the hydration degree with the assumed kinetic model for sample C20SZ.

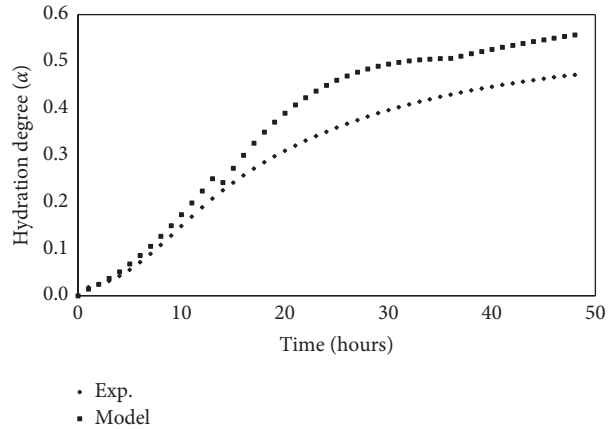

Figure 11: Experimental results of the hydration degree with the assumed kinetic model for sample C30SZ.

C10SZ and C20SZ, it is 28.42 h and 27.63 h. Sample C30SZ has a similar transition time $t_{I\text{-}D}$ as sample C.

The agreement of the experimental data α-t with the mathematical model is shown in Figures 8–11.

Considering the experimental data and the estimated kinetic model in Figure 8, the deviation of the model from the experimental data can be observed, especially in the area of the interaction between the phase boundaries. In Figures 9–11, this deviation is even greater, especially in the areas of interaction and diffusion. The proposed kinetic model can be applied to Portland cement without additives, while with the addition of saturated zeolite, some modifications of Jander's model should be conducted to ensure the scientific and accurate characterization of the hydration of cement [29, 30].

6. Conclusions

Based on the measurements and the obtained results, it can be concluded that the microcalorimetric method allows continuous monitoring and determination of the influence of saturated zeolite on the kinetic processes of hydration in the period of early hydration. After 48 hours of hydration, the total heat released shows that higher saturated zeolite content leads to lower heat values, while the occurrence of maximum hydration time occurs earlier. The rate of heat release and hydration degree decrease as the proportion of saturated zeolite in the sample increases. Significant deviations are observed between the measured and calculated values of the hydration degree when saturated zeolite is added to Portland cement, especially in later hydration times.

Data Availability

The data used to support the findings of this study are available from the corresponding author upon request.

Conflicts of Interest

The authors declare that they have no conflicts of interest.

References

[1] A. Bosoaga, O. Masek, and J. E. Oakey, "CO_2 capture technologies for cement industry," *Energy Procedia*, vol. 1, pp. 133–140, 2009.

[2] L. Poudyal and K. Adhikari, "Environmental sustainability in cement industry: an integrated approach for green and economical cement production," *Resources, Environment and Sustainability*, vol. 4, Article ID 100024, 2021.

[3] D. Wang, C. Shi, N. Farzadnia, Z. Shi, and H. Jia, "A review on effects of limestone powder on the properties of concrete," *Construction and Building Materials*, vol. 192, pp. 153–166, 2018.

[4] R. Siddique and J. Klaus, "Influence of metakaolin on the properties of mortar and concrete: a review," *Applied Clay Science*, vol. 43, no. 3–4, pp. 392–400, 2009.

[5] M. Shariq, J. Prasad, and A. K. Ahuja, "Strength development of cement mortar and concrete incorporating GGBFS," *Asian Journal of Civil Engineering*, vol. 9, no. 1, pp. 61–74, 2008.

[6] J. Skibsted and R. Snellings, "Reactivity of supplementary cementitious materials (SCMs) in cement blends," *Cement and Concrete Research*, vol. 124, Article ID 105799, 2019.

[7] V. J. Inglezakis and A. A. Zorpas, *Handbook of Natural Zeolites*, Bentham Books, Sharjah, UAE, 2012.

[8] N. A. A. Qasem, R. H. Mohammed, and D. U. Lawal, "Removal of heavy metal ions from wastewater: a comprehensive and critical review," *Npj Clean Water*, vol. 4, no. 1, 2021.

[9] S. Sharma and A. Bhattacharya, "Drinking water contamination and treatment techniques," *Applied Water Science*, vol. 7, no. 3, pp. 1043–1067, 2017.

[10] V. Albino, R. Cioffi, M. Pansini, and C. Colella, "Disposal of lead-containing zeolite sludges in cement matrix," *Environmental Technology*, vol. 16, no. 2, pp. 147–156, 1995.

[11] P. Dabić and D. Barbir, "Implementation of natural and artificial materials in Portland cement," *Chemical Industry*, vol. 74, no. 3, pp. 147–161, 2020.

[12] D. Barbir, P. Dabić, and A. Lisica, "Effects of mud from a zinc-plating plant and zeolite saturated with zinc on Portland cement hydration and properties of hardened cement pastes," *Chemical and Biochemical Engineering Quarterly Journal*, vol. 30, no. 4, pp. 401–409, 2017.

[13] P. C. Hewlett and M. Liska, *Lea's Chemistry of Cement and concrete*, Elsevier, Oxford, England, 2017.

[14] H. Zhang, *Building Materials in Civil Engineering*, Woodhead Publishing, Beijing, China, 2011.

[15] M. W. Bligh, M. N. d'Eurydice, R. R. Lloyd, C. H. Arns, and T. D. Waite, "Investigation of early hydration dynamics and microstructural development in ordinary Portland cement using 1H NMR relaxometry and isothermal calorimetry," *Cement and Concrete Research*, vol. 83, pp. 131–139, 2016.

[16] B. Klemczak and M. Batog, "Heat of hydration of low-clinker cements," *Journal of Thermal Analysis and Calorimetry*, vol. 123, no. 2, pp. 1351–1360, 2016.

[17] P. Šiler, I. Kolářová, R. Novotný et al., "Application of isothermal and isoperibolic calorimetry to assess the effect of zinc on hydration of cement blended with slag," *Materials*, vol. 12, no. 18, p. 2930, 2019.

[18] E. Pustovgar, R. P. Sangodkar, A. S. Andreev et al., "Understanding silicate hydration from quantitative analyses of hydrating tricalcium silicates," *Nature Communications*, vol. 7, no. 1, Article ID 10952, 2016.

[19] A. A. Elkordy, *Applications of Calorimetry in a Wide Context*, IntechOpen, Rijeka, Croatia, 2013.

[20] W. Nocuń-Wczelik, B. Trybalska, and E. Żugaj, "Application of calorimetry as a main tool in evaluation of the effect of carbonate additives on cement hydration," *Journal of Thermal Analysis and Calorimetry*, vol. 113, no. 1, pp. 351–356, 2013.

[21] R. Krstulović and P. Dabić, "A conceptual model of the cement hydration process," *Cement and Concrete Research*, vol. 30, no. 5, pp. 693–698, 2000.

[22] Y. Li, Y. Deng, and R. Liu, "Hydration kinetics of Portland cement–silica fume binary system at low temperature," *Materials*, vol. 12, no. 23, p. 3896, 2019.

[23] X. Y. Wang and H. S. Lee, "Modeling of hydration kinetics in cement based materials considering the effects of curing temperature and applied pressure," *Construction and Building Materials*, vol. 28, pp. 1–13, 2012.

[24] G. De Schutter, "Hydration and temperature development of concrete made with blast-furnace slag cement," *Cement and Concrete Research*, vol. 29, no. 1, pp. 143–149, 1999.

[25] X. Y. Wang, H. K. Cho, and H. S. Lee, "Prediction of temperature distribution in concrete incorporating fly ash or slag

using a hydration model," *Composites Part B: Engineering*, vol. 42, no. 1, pp. 27–40, 2011.

[26] H. Zhou, J. Liu, J. Liu, and C. Li, "Hydration kinetics process of low alkalinity sulphoaluminate cement and its thermodynamical properties," *Procedia Engineering*, vol. 27, pp. 323–331, 2012.

[27] M. Rožić, Š. Cerjan-Stefanović, S. Kurajica, M. R. Maěefat, K. Margeta, and A. Farkaš, "Decationization and dealumination of clinoptilolite tuff and ammonium exchange on acid-modified tuff," *Journal of Colloid and Interface Science*, vol. 284, no. 1, pp. 48–56, 2005.

[28] D. Barbir, *Studija Utjecaja Štetnih Otpada Na Procese Hidratacije I Fizikalno-Kemijska Te Mehanička Svojstva Cementnih Kompozita*, Doctoral thesis, Kemijsko-tehnološki fakultet, Split, Croatia, 2013.

[29] Z. Zhang, Y. Liu, L. Huang, and P. Yan, "A new hydration kinetics model of composite cementitious materials, part 1: hydration kinetic model of Portland cement," *Journal of the American Ceramic Society*, vol. 103, no. 3, pp. 1970–1991, 2020.

[30] Z. Zhang, W. Chen, F. Han, and P. Yan, "A new hydration kinetics model of composite cementitious materials, Part 2: physical effect of SCMs," *Journal of the American Ceramic Society*, vol. 103, no. 6, pp. 3880–3895, 2020.